PCCP

PAPER

View Article Online
View Journal | View Issue

Cite this: *Phys. Chem. Chem. Phys.*, 2019, **21**, 8092

The relationship between the asymmetric magnetoresistive effect and the magnetocaloric effect in $Ni_{43}Co_7Mn_{39-x}Cr_xSn_{11}$ Heusler alloys†

Yunli Xu, [a] Dongchao Yang,[a] Linjie Ding,[a] Lizhi Yi,[a] Shuaiwei Fan,[a] Liqing Pan, *[a] Jia Li,[b] Fengxia Hu, [b] Guanghua Yu[c] and John Q. Xiao *[d]

Received 9th January 2019,
Accepted 19th March 2019

DOI: 10.1039/c9cp00145j

rsc.li/pccp

The correlation between the magnetocaloric effect and magnetotransport property was investigated in $Ni_{43}Co_7Mn_{39-x}Cr_xSn_{11}$ Heusler alloys. The asymmetric isothermal-magnetoresistance around the phase transformation temperature was observed, from which a parameter γ, determined as the ratio of the asymmetric magnetoresistance to the temperature coefficient of resistance, is proposed. According to Maxwell's equation, the parameter γ is analyzed to be equivalent to the transformation temperature change induced by a magnetic field in martensitic transformation. This finding is confirmed by experimental results. In addition, the γ values can be used to estimate the magnetic entropy change of the martensitic transformation directly without measuring the comprehensive temperature dependence of magnetization curves.

1. Introduction

Heusler alloys with magnetic-field-induced phase transformation exhibit many novel effects, such as the shape memory effect induced by a magnetic field,[1] magnetoelastic effect,[2–4] giant magnetoresistance (MR),[5] magnetocaloric effect (MCE),[6] refrigeration capacity,[7] exchange bias, *etc.*[4,8–11] In the past decades, Ni–Co–Mn–Sn alloys have attracted much attention due to their giant MCE and giant MR effect during phase transformation. Huang L. *et al.* reported an entropy change of 14.9 J kg^{-1} K^{-1} for the $Ni_{40}Co_{10}Mn_{40}Sn_{10}$ bulk alloy under 5 T.[7] For $Ni_{40}Co_{10}Mn_{40}Sn_{10}$ powders, it is 27 J kg^{-1} K^{-1} as reported by Wang X. L. *et al.*[6] Nb-Doping can effectively improve the entropy change of Ni–Co–Mn–Sn alloys. For instance the entropy change reaches 41.4 J kg^{-1} K^{-1} for $Ni_{44}Nb_1Co_5Mn_{40}Sn_{10}$ under 7 T. Although a small amount of Nb doping can increase the entropy change of Ni–Co–Mn–Sn alloys, the latent heat of the martensitic transition decreases.[12] Large symmetric MR values of −69%,[13] −59%[15] and −40%[14] have also been reported for Ni–Co–Mn–Sn alloys.[16] Dubenko I. *et al.* reported an asymmetric MR in the vicinity of the martensitic transformation, and they infer that the asymmetric MR could be related to the kinetic arrest and de-arrest of a fractional austenite phase in the martensitic transformation.[17] Samanta T. *et al.* observed an asymmetric switching-like magnetoresistance in a B-substituted Ni–Mn–In Heusler alloy, which originates from the asymmetry between the forward and reverse metamagnetic transitions.[18] Rodionov I. D. *et al.* studied the correlation between the magnetic part of the entropy and magnetoresistance, and concluded that no universal correlation exists between these effects.[19] In all these works, the relationship between asymmetric MR and the MCE has not been studied, which is the purpose of this manuscript. We found a new parameter γ that, determined from the magnetotransport property, can be used to characterize the change of the magnetic-field-induced transformation temperature. In addition, this parameter γ can also be used to estimate the entropy changes without measuring the comprehensive temperature dependence of magnetic hysteresis loops.

2. Experiments

Samples with nominal compositions of $Ni_{43}Co_7Mn_{39-x}Cr_xSn_{11}$, x = 0, 0.5, 1 and 1.5, were synthesized by arc-melting the high-purity elemental metals (Ni, 99.995%; Co, 99.95%; Mn, 99.99%; Cr, 99.999%; and Sn, 99.999%) under an Ar atmosphere. The base pressure was less than 10^{-4} Pa. To compensate for the mass loss during arc melting, an excess of 2 wt% of Mn was added.

[a] *Research Institute for Magnetoelectronics & Weak Magnetic-Field Detection, College of Science, China Three Gorges University, Yichang 443002, China. E-mail: lpan@ctgu.edu.cn*
[b] *State Key Laboratory of Magnetism, Institute of Physics, Chinese Academy of Science, Beijing 100190, China*
[c] *School of Materials Science and Engineering, University of Science and Technology Beijing, Beijing 100083, China*
[d] *Department of Physics and Astronomy, University of Delaware, Newark, DE, 19716, USA. E-mail: jqx@udel.edu*

† Electronic supplementary information (ESI) available. See DOI: 10.1039/c9cp00145j

All samples were melted 4–5 times under magnetic stirring, and turned over during each iteration to ensure sample homogeneity. The obtained samples were annealed at 1173 K for 24 h in evacuated quartz tubes before being quenched into an ice water bath. Finally, the obtained samples were ground and cut into different shapes by wire cutting for testing.

The crystalline structure characterization was performed using an X-ray powder diffractometer (D8 Advance, Bruker Corp., USA) with Cu Kα radiation. The chemical composition of the alloys was determined by energy-dispersive X-ray spectroscopy (EDS) (Quanta 200, ThermoFisher Scientific, USA). The magnetic properties and phase transformation measurements were carried out using a mini-physical property measurement system (VersaLab, Quantum Design, USA) under a magnetic field of up to 3 T and using a physical property measurement system (Quantum Design, USA) under a magnetic field up of to 7 T. The MR curves were measured using the ETO mode in the VSM with a standard four-probe method on a sample strip of 10 mm × 2 mm × 0.5 mm.

3. Results and discussion

3.1 MCE

All samples with different Cr concentrations show a similar behavior. We therefore focus our discussion on a representative sample of $Ni_{43}Co_7Mn_{38}Cr_1Sn_{11}$ alloys. Fig. 1(a) shows the thermomagnetization curves of the alloy. With a 1% Cr dopant, the starting temperature (T_M) for martensitic transformation decreases to 250 K under 1 T magnetic field, which is about 60 K lower than that of $Ni_{43}Co_7Mn_{39}Sn_{11}$ without a Cr dopant. The magnetization difference (ΔM) between the parent phase and martensite reaches 80 A m^2 kg^{-1} at 1 T magnetic field.

The magnetic behaviors around the MT temperature can reveal the state of the magnetic order. Fig. 1(b) shows the hysteresis loops of the $Ni_{43}Co_7Mn_{38}Cr_1Sn_{11}$ alloy at different temperatures near the MT. The hysteresis loops below 230 K show typical weak magnetic behavior, whereas the loop at 270 K shows ferromagnetic behavior. The hysteresis loops exhibit obvious magnetic-field-induced metamagnetic behavior from 240 K to 255 K. The magnetization increases rapidly under a low field and then forms a huge hysteresis loop in the plateau region with increasing and decreasing magnetic field. This behavior is a typical feature of the MT induced by the magnetic field.[20] Note that the loops at 240–255 K are not completely closed at 3 T, indicating that the Zeeman energy at 3 T is not strong enough to complete the MT. The inset of Fig. 1(b) shows that the coercivity is less than 50 Oe at each temperature.

The X-ray diffraction (XRD) patterns at different temperature are shown in Fig. 1(c). The sample shows a cubic austenite phase at 285 K. With the decrease of temperature, the structure evolves into a modulated martensite phase at 150 K, which indicates a temperature-induced phase transformation, consistent with the observed magnetic field-induced phase transformation.

Fig. 2(a) shows the isothermal M–H curves measured in the vicinity of the phase transition. A large magnetic entropy change (ΔS) associated with the first-order magnetostructural transition can be calculated by the Maxwell relation based on the M–H curves:

$$\Delta S = S_m(T,H) - S_m(T,0) = \int_0^{\mu_0 H} \frac{\partial M}{\partial T} d(\mu_0 H) \qquad (1)$$

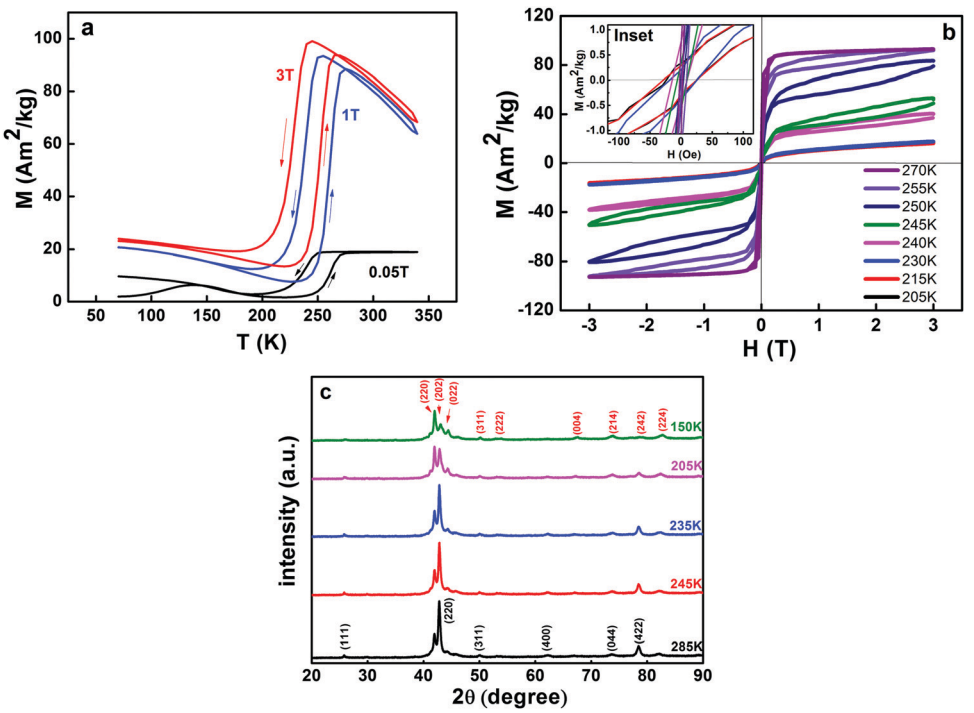

Fig. 1 (a) Thermomagnetization curves of the $Ni_{43}Co_7Mn_{38}Cr_1Sn_{11}$ alloy. (b) Magnetic hysteresis loops of the same alloy at different temperatures near the MT temperature. The inset shows the enlarged loops near zero field. (c) Diffraction patterns at different temperatures of the same alloy.

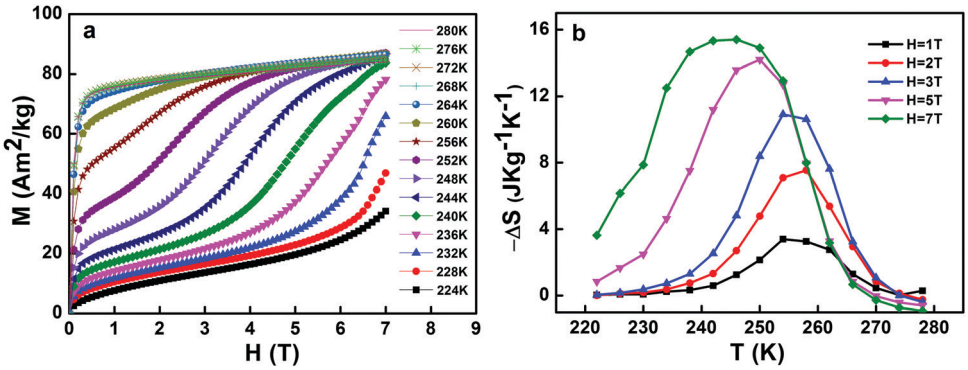

Fig. 2 (a) The isothermal $M(H)$ curves at constant temperature from 224 K to 280 K. (b) The magnetic entropy change (ΔS) under magnetic field as a function of temperature.

Fig. 2(b) illustrates the temperature dependence of ΔS under different magnetic fields. The peak value of ΔS increases with increasing magnetic field. The maximum value of ΔS calculated under 7 T is about -15.4 J kg^{-1} K^{-1}.

3.2 Magnetotransport properties

Fig. 3(a) shows the MR behaviors of a $Ni_{43}Co_7Mn_{38}Cr_1Sn_{11}$ alloy under a magnetic field at different temperatures around the MT. For clarity we only show data in the field swept from -3 T to 3 T, which is symmetric to those from 3 T to -3 T. The MR in the range of 205–230 K is nearly symmetric. As the temperature rises, the MR decreases further and the MR curves become distinctly asymmetric with respect to zero field. The resistance difference between zero and maximum fields reaches a peak at 250 K, then decreases with a further increase in the temperature, and finally vanishes at 270 K.

Fig. 3(b) shows the temperature dependence of the resistance of the $Ni_{43}Co_7Mn_{38}Cr_1Sn_{11}$ alloy measured at $H = 0$ T. The powder XRD and TEM experiments confirmed that the parent phase has a $L2_1$ Heusler-type ordered structure with a = 0.5965 nm, and the martensite phase is a mixture of 10 M and 6 M modulated structures where the crystalline structure parameters are a = 0.4319 nm, b = 0.2747 nm, c = 2.109 nm, and $\beta = 90.64^\circ$ for 10 M modulated martensite.[2,24] The distortion of the structure from a cubic to a monoclinic crystal during the martensitic transformation elongates the c axis of the unit cell. Consequently, the densities of states at the Fermi levels decrease, which leads to the increase of the resistance as shown in Fig. 3(b). The resistance loops reflect the temperature hysteresis of the MT. The red/black lines denote the heating/cooling processes, respectively. We used the cooling process to calculate dR/dT and to measure the R–H curves.

Fig. 4(a) shows the magnetoresistance curve of the sample at 250 K. There is a significant difference in resistance between the increasing and decreasing fields, which is related to the magnetic-field-induced phase transformation. Since the magnetic coercivity of the $Ni_{43}Co_7Mn_{38}Cr_1Sn_{11}$ alloy is less than 50 Oe, the effect of magnetic hysteresis on magnetoresistance can be neglected.

3.3 Relationship between MR and the MCE

The MR effect for the metamagnetic Heusler alloys near the phase transition includes two parts: the common MR and the structure-induced change of resistance by the magnetic-field-induced MT effect. MR can be expressed as:

$$\Delta R = \Delta R(H) + \Delta R(S) \quad (2)$$

where $\Delta R(H)$ is the common MR without structural transformation and $\Delta R(S)$ is the resistance variation resulting from the structural change.

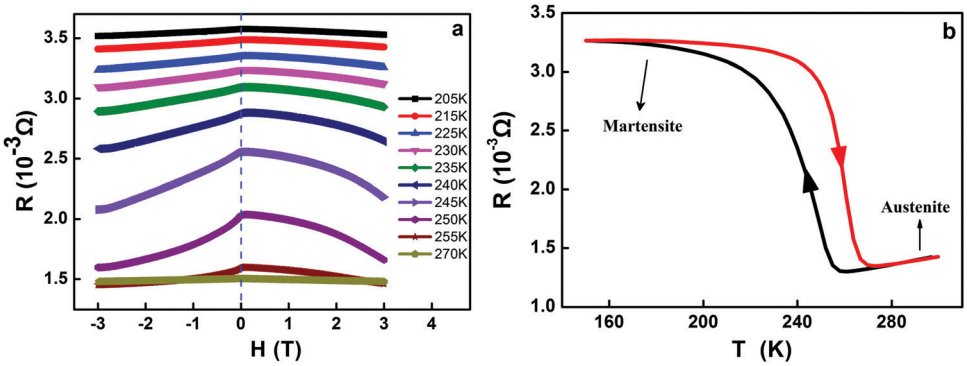

Fig. 3 (a) Magnetoresistance as a function of magnetic field at different temperatures. (b) The temperature dependence of the resistance under zero magnetic field.

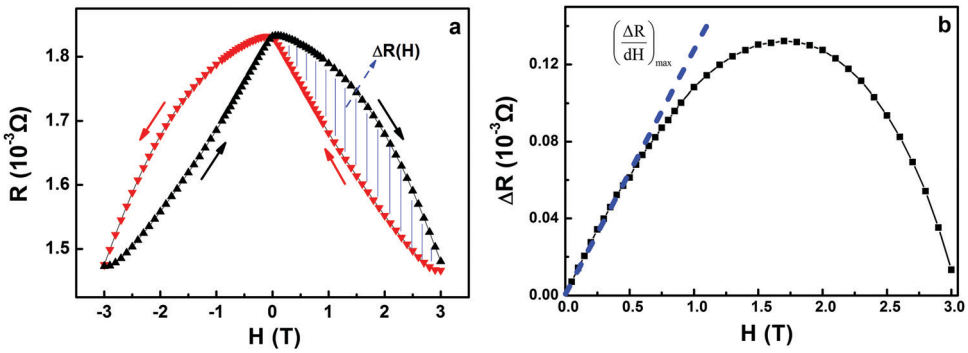

Fig. 4 (a) Magnetoresistance curve at 250 K. (b) Magnetic field dependence of the change of the resistance between the increasing and decreasing fields (ΔR in Fig. 3(a)) at 250 K.

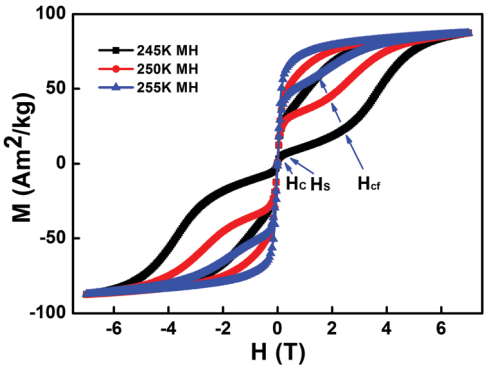

Fig. 5 Magnetic hysteresis loops of the $Ni_{43}Co_7Mn_{38}Cr_1Sn_{11}$ alloy at 245 K, 250 K, and 255 K, respectively, where H_c is the coercive field, H_s is the saturation field and H_{cf} is the critical field of magnetic-field-induced phase transformation.

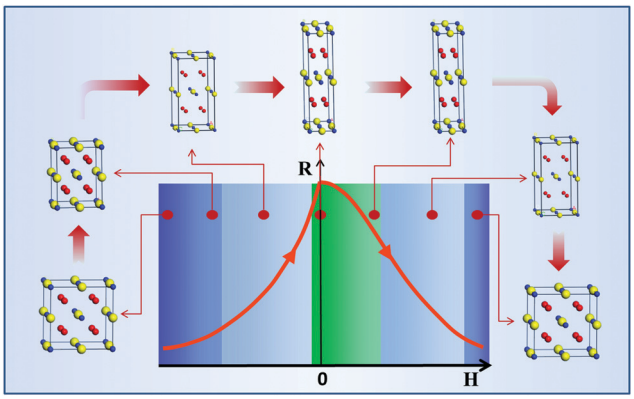

Fig. 6 The schematic diagram of the $Ni_{43}Co_7Mn_{38}Cr_1Sn_{11}$ alloy structural change under a magnetic field from a negative to positive magnetic field.

The unclosed hysteresis loops in Fig. 1(b) indicate that the Zeeman energy under a magnetic field of 3 T is not high enough to complete MT for the $Ni_{43}Co_7Mn_{38}Cr_1Sn_{11}$ alloy. If the magnetic field is high enough to complete the phase transformation, the magnetization of the alloy will increase sharply as shown in Fig. 5, in which we define the on-set critical field H_{cf} when the magnetization starts to rise rapidly. There is a large difference between the critical field H_{cf} and the saturation field H_s, both are much larger than the coercivity H_c. In a large field range of $H_c \ll H \ll H_{cf}$, we can distinguish the origin of MR, which comes from $\Delta R(H)$ and $\Delta R(S)$. We schematically illustrate the process from a negative to positive magnetic field in Fig. 6.

Starting from −3 T, the variation of the resistance can be expressed as $\Delta R_1 = \Delta R(H) + \Delta R(S)$, corresponding to the austenite phase. Upon reducing the field from −3 T to 0, the Zeeman energy is released slowly and the structure of the alloy recovers gradually to the martensite phase in zero field. As the magnetic field is increased from 0 to 3 T, the change of the MR undergoes two stages: (1) the Zeeman energy of a small magnetic field is low, which is unable to drive any structural phase transformation. The MR only comes from a single source: $\Delta R_2 = \Delta R(H)$. The spin dependent scattering decreases with increasing field, leading to the decrease of the resistance; (2) the magnetic field increases to the critical value of H_{cf}, which triggers the magnetic-field-induced inverse phase transformation, driving the structure from martensite to austenite. Therefore the MR comes from both sources and can be expressed as: $\Delta R_3 = \Delta R(H) + \Delta R(S)$. Under the high field, the MR curve gradually becomes symmetric with $\Delta R_3 = \Delta R_1$.

Since the MR is intimately related to the phase transformation, we defined a new scaling factor γ as:

$$\gamma = \left(\frac{\Delta R}{dH}\right)_{max} \Big/ \left(\frac{dR}{dT}\right) \quad (3)$$

where $\left(\frac{\Delta R}{dH}\right)_{max}$ is the asymmetric magnetoresistance, defined in Fig. 4(b).

To illustrate the meaning of γ, we analyze the components of the full differential of resistance. The resistance R is a function of magnetic field H and temperature T. The full differential of $R(H,T)$ can be expressed as follows:

$$dR = \left(\frac{\partial R}{\partial T}\right)_H dT + \left(\frac{\partial R}{\partial H}\right)_T dH \quad (4)$$

or

$$\frac{dR}{dH} = \left(\frac{\partial R}{\partial T}\right)_H \frac{dT}{dH} + \left(\frac{\partial R}{\partial H}\right)_T \quad (5)$$

Therefore, the complete differential of resistance subtracts the change only from the magnetic field is equal to:

$$\frac{dR}{dH} - \left(\frac{\partial R}{\partial H}\right)_T = \left(\frac{\partial R}{\partial T}\right)_H \cdot \frac{dT}{dH} \quad (6)$$

The left side of eqn (6) is the abovementioned $\left(\frac{\Delta R}{dH}\right)_{max}$. Compared to the right side of eqn (6), we have obtained

$$\gamma = \frac{dT}{dH} \quad (7)$$

In addition, in an adiabatic process, the change of entropy is zero.

$$dS = \left(\frac{\partial S}{\partial T}\right)_H dT + \left(\frac{\partial S}{\partial H}\right)_T dH = 0 \quad (8)$$

Therefore

$$\left(\frac{dT}{dH}\right)_S = -\frac{\left(\frac{\partial S}{\partial H}\right)_T}{\left(\frac{\partial S}{\partial T}\right)_H} \quad (9)$$

Using the Maxwell relation, we obtain:

$$\left(\frac{\partial S}{\partial H}\right)_T = \left(\frac{\partial M}{\partial T}\right)_H \quad (10)$$

Eqn (9) and (10) lead to:

$$\left(\frac{dT}{dH}\right)_S = -\frac{\left(\frac{\partial M}{\partial T}\right)_H}{\left(\frac{\partial S}{\partial T}\right)_H} = -\left(\frac{\partial M}{\partial S}\right)_H \quad (11)$$

which is the Clausius–Clapeyron equation.[5]

Therefore, eqn (6) can also be expressed as:

$$\frac{dR}{dH} - \left(\frac{\partial R}{\partial H}\right)_T = -\left(\frac{\partial R}{\partial T}\right)_H \left(\frac{\partial M}{\partial S}\right)_H \quad (12)$$

From eqn (7), γ represents the phase transformation temperature change induced by the magnetic field. It also reflects the value of $-\frac{\Delta M}{\Delta S}$ for the MT.

Fig. 7 shows $-\gamma$ of the $Ni_{43}Co_7Mn_{38}Cr_1Sn_{11}$ alloy calculated from eqn (3). The value of $-\gamma$ reaches a maximum value of 5.3 K T^{-1} at 250 K and then decreases rapidly with increasing temperature and reaches zero at 270 K. The value of $-\gamma$ approaches zero after the structure of the alloy has transformed into austenite, consistent with the mechanism of magnetic-field-induced phase transformation. Combined with the thermomagnetization curves in Fig. 1(a), the magnetostructural-coupling phase transformation of the alloy is proved. Moreover, the value of $\frac{dT}{dH}$ can also be calculated from the transformation temperatures under different applied magnetic fields. For instance, at H = 1 T and H = 3 T, shown in the thermomagnetization curves in Fig. 1(a), $\frac{dT}{dH} = -5$ K T^{-1} was obtained, which is equal to the calculated value using eqn (3).

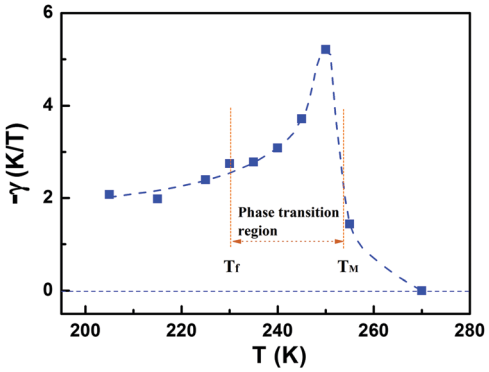

Fig. 7 The temperature dependence of γ of the $Ni_{43}Co_7Mn_{38}Cr_1Sn_{11}$ alloy. T_M: martensitic transformation onset temperature, T_f: martensitic transformation finish temperature.

The equivalent transformation temperature change induced by the magnetic field is generally given by the Clausius–Clapeyron equation:[20]

$$\frac{dT}{dH} = -\frac{\Delta M}{\Delta S} \quad (13)$$

where ΔM is the magnetization difference between the martensitic and austenite phases, and ΔS is the entropy change. From previous studies,[21] the value of $-dT/dH$ is only 2 K T^{-1} for the $Ni_{50}Mn_{35}In_{15}$ alloy and up to 12 K T^{-1} for the $Ni_{50}Mn_{34}In_{16}$ alloy. In this work for the $Ni_{43}Co_7Mn_{38}Cr_1Sn_{11}$ alloy, the value of $-dT/dH$ is calculated to be 5.06 K T^{-1} using eqn (13) according to ΔS = 15.4 J kg^{-1} K^{-1} obtained experimentally at 7 T as shown in Fig. 2(b), which is very close to $-\gamma$ = 5.3 K T^{-1} calculated using eqn (3). Conversely, if the values of $-\gamma$ and ΔM are known, the magnetic entropy change can be calculated directly using the Clausius–Clapeyron equation (eqn (13)), and comprehensive magnetization curves at variable temperature need not be measured except for a M–T curve taken at sufficiently high magnetic field for measuring ΔM. For example, in the case of the $Ni_{43}Co_7Mn_{38}Cr_1Sn_{11}$ alloy, the values of ΔM = 78 A m^2 kg^{-1} and $-\gamma$ = 5.3 K T^{-1} lead to ΔS = 14.7 J kg^{-1} K^{-1} according to eqn (13). The value is very close to the result of our experiment.

To verify the effectiveness of eqn (3), we have calculated the data in ref. 22 and 23. The calculated γ is 5.71 (K T^{-1}). $\frac{dT}{dH} = -\frac{\Delta M}{\Delta S} = 4.85$ K T^{-1} is obtained from eqn (13), which is close to the value of γ. Since the thermomagnetization curve at 6 T was not given in ref. 22 and 23, we just use the data at 290 K and 240 K to calculate ΔM. The magnitude of ΔM may be slightly smaller than the actual value, which results in a smaller value of $\Delta M/\Delta S$. The above calculation process is detailed in the Supplementary materials 2, ESI.†

For samples with different Cr concentrations, their compositions have been determined by EDS. The actual Co and Cr contents are about 10% smaller than the nominal composition whereas other elements slightly fluctuate around the nominal compositions. The various parameters for other samples in a $Ni_{43}Co_7Mn_{39-x}Cr_xSn_{11}$ series are shown in Table 1 (see details

Table 1 The magnetization of the austenite (M_A) and martensite (M_M) phases, dT/dH and γ of all samples

Sample	M_A (emu g^{-1})	M_M (emu g^{-1})	dT/dH (K T^{-1})	γ (K T^{-1})	Origin
$Ni_{43}Co_7Mn_{39}Sn_{11}$	74	16	2.3	2.11	This work
$Ni_{43}Co_7Mn_{38.5}Cr_{0.5}Sn_{11}$	74	7.4	3.25	1.97	This work
$Ni_{43}Co_7Mn_{38}Cr_1Sn_{11}$	98	20	5.0	5.3	This work
$Ni_{43}Co_7Mn_{37.5}Cr_{1.5}Sn_{11}$	106	53	6.6	6.4	This work
$Ni_{42}Co_8Mn_{32}Al_{18}$	—	—	4.85	5.71	Ref. 22 and 23

in the ESI†). The parameter γ and dT/dH are consistent with each other.

4. Conclusions

The relationship between asymmetric MR and the MCE has been studied by Maxwell's relations and the Clausius–Clapeyron equations, and verified experimentally. In the vicinity of the phase transformation of the $Ni_{43}Co_7Mn_{39-x}Cr_xSn_{11}$ alloys, the asymmetric MR has been observed, which corresponds to the magnetostructural transformation. We propose a new factor γ, which can be determined from the magnetotransport properties, and prove that it is equivalent to the transformation temperature change induced by the magnetic field. This factor γ can also be used to estimate the magnetic entropy of the martensitic transformation.

Conflicts of interest

There are no conflicts to declare.

Acknowledgements

The author Y. L. Xu thanks Mr Cheng Chen for the help in the magneto-transport measurement. This work was supported by the National Natural Science Foundation of China (Grant No. 51371105, 11474183 and 51501102). J. Q. X. is supported by NSF grant DMR1505592.

References

1 F. Chen, Y. X. Tong, B. Tian, L. Li and Y. F. Zheng, Martensitic transformation and magnetic properties of Ti-doped NiCoMnSn shape memory alloy, *Rare Met.*, 2014, **33**(5), 511–515.

2 R. Kainuma, Y. Imano, W. Ito, H. Morito, Y. Sutou, K. Oikawa, A. Fujita, K. Ishida, S. Okamoto, O. Kitakami and T. Kanomata, Metamagnetic shape memory effect in a Heusler-type $Ni_{43}Co_7Mn_{39}Sn_{11}$ polycrystalline alloy, *Appl. Phys. Lett.*, 2006, **88**, 19.

3 N. M. Bruno, C. Yegin, I. Karaman, J.-H. Chen, J. H. Ross, J. Liu and J. Li, The effect of heat treatments on $Ni_{43}Mn_{42-}Co_4Sn_{11}$ meta-magnetic shape memory alloys for magnetic refrigeration, *Acta Mater.*, 2014, **74**(4), 66–84.

4 Z. Yang, D. Y. Cong, L. Huang, Z. H. Nie, X. M. Sun, Q. H. Zhang and Y. D. Wang, Large elastocaloric effect in a Ni–Co–Mn–Sn magnetic shape memory alloy, *Mater. Des.*, 2015, **92**, 932–936.

5 G. H. Yu, Y. L. Xu, Z. H. Liu, H. M. Qiu, Z. Y. Zhu, X. P. Huang and L. Q. Pan, Recent progress in Heusler-type magnetic shape memory alloys, *Rare Met.*, 2015, **34**, 527–539.

6 X. Wang, F. Sun, J. Wang, Q. Yu, Y. Wu, H. Hua and C. Jiang, Influence of annealing temperatures on the magnetostructural transformation and magnetocaloric effect of $Ni_{40}Co_{10}Mn_{40}Sn_{10}$ powders, *J. Alloys Compd.*, 2017, **691**, 215–219.

7 L. Huang, D. Y. Cong, H. L. Suo and Y. D. Wang, Giant magnetic refrigeration capacity near room temperature in $Ni_{40}Co_{10}Mn_{40}Sn_{10}$ multifunctional alloy, *Appl. Phys. Lett.*, 2014, **104**(13), 132407.

8 M. Halder, M. D. Mukadam, K. G. Suresh and S. M. Yusuf, Electronic, structural, and magnetic properties of the quaternary Heusler alloy NiCoMnZ (Z = Al, Ge, and Sn), *J. Magn. Magn. Mater.*, 2015, **377**, 220–225.

9 A. Çakır, M. Acet, U. Wiedwald, T. Krenke and M. Farle, Shell-ferromagnetic precipitation in martensitic off-stoichiometric Ni-Mn-In Heusler alloys produced by temper-annealing under magnetic field, *Acta Mater.*, 2017, **127**, 117–123.

10 V. Srivastava, X. Chen and R. D. James, Hysteresis and unusual magnetic properties in the singular Heusler alloy $Ni_{45}Co_5Mn_{40}Sn_{10}$, *Appl. Phys. Lett.*, 2010, **97**(1), 159.

11 S. C. Ma, H. C. Xuan, C. L. Zhang, L. Y. Wang, Q. Q. Cao, D. H. Wang and Y. W. Du, Investigation of the intermediate phase and magnetocaloric properties in high-pressure annealing Ni–Mn–Co–Sn alloy, *Appl. Phys. Lett.*, 2010, **97**(5), 1746.

12 B. Emre, N. M. Bruno, E. S. Yuce and I. Karaman, Effect of niobium addition on the martensitic transformation and magnetocaloric effect in low hysteresis NiCoMnSn magnetic shape memory alloys, *Appl. Phys. Lett.*, 2014, **105**, 23.

13 A. Ghosh and K. Mandal, Large magnetoresistance associated with large inverse magnetocaloric effect in Ni-Co-Mn-Sn alloys, *Eur. Phys. J. B*, 2013, **86**(9), 1–6.

14 Z. H. Liu, Z. G. Wu, X. Q. Ma, W. H. Wang, Y. Liu and G. H. Wu, Large magnetization change and magnetoresistance associated with martensitic transformation in $Mn_2Ni_{1.36}Sn_{0.32}Co_{0.32}$ alloy, *J. Appl. Phys.*, 2011, **110**(1), 957.

15 Z. D. Han, D. H. Wang, B. Qian, J. F. Feng, X. F. Jiang and Y. W. Du, Phase Transformations, Magnetocaloric Effect and Magnetoresistance in Ni-Co-Mn-Sn Ferromagnetic Shape Memory Alloy, *Jpn. J. Appl. Phys.*, 2010, **49**(1), 0211.

16 T. Graf, C. Felser and S. S. P. Parkin, Simple rules for the understanding of Heusler compounds, *Prog. Solid State Chem.*, 2011, **39**, 1–50.

17 I. Dubenko, T. Samanta, A. Quetz, A. Saleheen, V. N. Prudnikov, A. B. Granovsky, S. Stadler and N. Ali, Asymmetric magnetoresistance in bulk In-based off-stoichiometric Heusler alloys, *Phys. Status Solidi A*, 2014, **11**(5-6), 1000–1003.

18 T. Samanta, A. U. Saleheen, D. L. Lepkowski, A. Shankar and S. Stadler, Asymmetric switchinglike behavior in the magnetoresistance at low fields in bulk metamagnetic heusler alloys, *Phys. Rev. B: Condens. Matter Mater. Phys.*, 2014, **90**(6), 064412.

19 I. D. Rodionov, D. E. Mettus, A. P. Kazakov, M. V. Prudnikova, V. N. Prudnikov and I. S. Dubenko, *et al.*, Correlation

between magnetoresistance and magnetic entropy at first-order and second-order phase transitions in ni-mn-in-si heusler alloys, *Phys. Solid State*, 2013, **55**(9), 1861–1865.

20 R. Kainuma, Y. Imano, W. Ito, Y. Sutou, H. Morito, S. Okamoto, O. Kitakami, K. Oikawa, A. Fujita, T. Kanomata and K. Ishida, Magnetic-field-induced shape recovery by reverse phase transformation, *Nature*, 2006, **439**, 7079.

21 S. Y. Yu, Z. H. Liu, G. D. Liu, J. L. Chen, Z. X. Cao and G. H. Wu, Large magnetoresistance in single-crystalline $Ni_{50}Mn_{50-x}In_x$ alloys (x = 14–16) upon martensitic transformation, *Appl. Phys. Lett.*, 2006, **89**, 162503.

22 H. C. Xuan, L. J. Shen, T. Tang, Q. Q. Cao, D. H. Wang and Y. W. Du, Magnetic-field-induced reverse martensitic transformation and large magnetoresistance in $Ni_{50-x}Co_xMn_{32}Al_{18}$ Heusler alloys, *Appl. Phys. Lett.*, 2012, **100**, 172410.

23 H. C. Xuan, F. H. Chen, P. D. Han, D. H. Wang and Y. W. Du, Effect of Co addition on the martensitic transformation and magnetocaloric effect of Ni-Mn-Al ferromagnetic shape memory Alloys, *Intermetallics*, 2014, **47**, 31–35.

24 S. Morito, T. Kakeshita, K. Hirata and K. Otsuka, Magnetic and martensitic transformations in $Ni_{50}Al_xMn_{50-x}$ alloys, *Acta Mater.*, 1998, **46**(15), 5377–5384.

